Direct Imaging of Domain Wall Interactions in $Ni_{80}Fe_{20}$ Planar Nanowires

T.J. Hayward[1], M.T. Bryan[1], P.W. Fry[2], P.M. Fundi[1], M.R.J. Gibbs[1], D.A. Allwood[1], M.-Y. Im[3] and P. Fischer[3]

[1]*Department of Engineering Materials, University of Sheffield, Sheffield, UK*

[2]*Nanoscience and Technology Centre, University of Sheffield, Sheffield UK*

[3]*Center for X-ray Optics, Lawrence Berkeley Natl Lab, Berkeley, CA, USA*

PACS: 07.85.Tt, 75.60.Ch, 75.75.+a, 85.70.Kh

We have investigated magnetostatic interactions between domain walls in $Ni_{80}Fe_{20}$ planar nanowires using magnetic soft X-ray microscopy and micromagnetic simulations. In addition to significant monopole-like attraction and repulsion effects we observe that there is coupling of the magnetization configurations of the walls. This is explained in terms of an interaction energy that depends not only on the distance between the walls, but also upon their internal magnetization structure.

The properties of domain walls (DWs) confined within planar ferromagnetic nanowires [1] are currently of great research interest. These DWs represent a well-defined nanomagnetic system that is ideal for fundamental studies and have particle-like properties that allow them to be propagated controllably around nanowire circuits in a manner analogous to the movement of electrical charge in standard microelectronics. This has led to designs for memory [2] and logic devices [3] that use DWs to separate binary data, represented by uniformly magnetized domains.

Despite a large body of work investigating the structure [1,4,5], propagation [6-9] and pinning [10-12] of DWs in nanowires, few studies have examined interactions between them [13,14]. The magnetization of a nanowire lies predominantly along its length to minimize magnetostatic energy. Consequently, DWs are boundaries between either converging ('head-to-head'; H2H) or diverging ('tail-to-tail'; T2T) magnetization [Fig. 1(a)], and carry an intrinsic magnetic monopole moment (North or South). Coulomb-like interactions between these effective monopole moments may be complicated when nanowires are in close proximity by DWs having non-uniform magnetization configurations ("vortex" [Fig. 1(b)] and "transverse" [Fig. 1(c)]) in which the chirality of the magnetization rotation may also vary. Understanding these interactions is therefore a non-trivial physical problem, requiring a detailed knowledge of how the DWs' complex magnetization structures both create and respond to highly non-uniform magnetic fields. Thus far, these features have not been fully

characterized, and must be studied experimentally or by numerical simulations, due to the difficulty of applying simple analytical treatments to a system with so many degrees of freedom. Such a study is not only interesting from the perspective of fundamental physics, but will also be important in the design of future devices where a high density of nanowires is desirable.

Here, we present magnetic X-ray imaging and micromagnetic modeling results that demonstrate strong attraction/repulsion between DWs with opposite/like monopole moments and additional coupling that depends on the detailed magnetization configurations of the two walls.

Pairs of 440 nm wide magnetic nanowires were fabricated from 33 nm thick $Ni_{80}Fe_{20}$ films on Si_3N_4 membranes using electron-beam lithography and lift-off processing. The nanowires were semi-circular in shape, such that saturation in a radial direction followed by relaxation created a bi-domain state consisting of two circumferential domains separated by a H2H or T2T DW. Two different pair geometries were fabricated: in the "mirror" geometry, the two wires curve in opposite directions [Fig. 1(d)] and hence DWs with opposite monopole moments are created following saturation (i.e. North and South). In the "concentric" geometry, the wires curve in the same direction [Fig. 1(e)], and DWs with like monopole moments are formed (i.e. either both North and both South). In each pair of wires the right-hand wire contained a notch at its apex in order to create a well-defined DW pinning site. The wires were separated by distances d = 50 nm, 100 nm and 200 nm for the mirror geometry, and d = 150 nm, 200 nm and 500 nm for the concentric geometry.

Magnetic transmission X-ray microscopy (M-TXM) at the Fe L_3 (706 eV) absorption edge was performed at beamline 6.1.2 at the Advanced Light Source in Berkeley CA [15,16]. The X-ray optics provided a high spatial resolution better than 25nm, which was essential for our experimental studies. In-plane magnetic contrast was achieved by differential imaging with left and right circularly polarized X-rays, with the sample tilted at 30° to normal incidence. Magnetic fields could be applied along the sample plane both parallel and perpendicular to the direction of magnetic contrast. To investigate interactions between DWs each pair of wires was repeatedly saturated using fields of ± 1 kOe, relaxed and imaged. The positions and structures of the two DWs formed in the wires were analyzed following each reversal.

Micromagnetic simulations were performed using the OOMMF software package [17]. The simulations were performed on a 2D mesh composed of 5 nm x 5 nm cells. Standard parameters were used to represent the material constants of $Ni_{80}Fe_{20}$ (M_S = 860 kA/m, A = 13 pJ/m, K_1 = 0).

X-ray images of DWs in isolated wires showed that the vortex wall structure was favored, as expected from the wires' large dimensions [1,4]. Micromagnetic simulations supported this, showing that a transverse wall had energy 16 % higher than a vortex wall.

All of the wall pairs observed in wires with the mirror geometry [e.g. Figs. 2(a)-(c)] were aligned with low displacements from each other, such that the wall centers were separated by a lateral distance no greater than half the apparent vortex wall width. This is consistent with the walls experiencing an attractive interaction due to their opposite magnetic polarity. However, a large majority of DW pairs in the concentric wire geometry (56 of the 62 wall pairs observed) were separated by at least half the vortex wall width [e.g. Figs. 2(d)-(f)]. This is consistent with the like-monopole domain walls experiencing a repulsive interaction. Furthermore, the more closely spaced pairs of walls in the concentric geometry were only observed with larger wire spacing (d = 200 nm, 500 nm), where weaker DW interactions made defects more significant in determining wall positions. The average values of the wall displacements observed in the concentric geometry wire pairs were 984 nm (d = 150 nm), 877 nm (d = 200 nm) and 541 nm (d = 500 nm), again demonstrating the weakening of the DW interaction strength with increasing d.

In addition to the simple attraction/repulsion effects described above, strong correlation between the structure and chirality of neighboring DWs was also observed. At d = 50 nm, DW pairs in the mirror wires had parallel transverse structures [Fig. 2(a)]. Micromagnetic simulations showed this configuration to be meta-stable, with energy 3.6 % higher than the ground state of two vortex walls with identical chirality. We believe that the meta-stable transverse wall was observed preferentially because it was formed as a precursor to the vortex wall as the wires relaxed from saturation. The magnetic flux closure between the opposite monopole moments of the DWs is aligned in the same direction as the transverse magnetization of the transverse walls and hence creates an energy barrier against the twisting required to form a vortex wall.

With d = 100 nm, the mirror wires exhibited pairs of transverse walls and pairs of vortex walls with identical circulations in successive relaxations [Fig. 2(b)]. The interaction between the walls was weaker, and could no longer reliably stabilize the transverse wall configurations. The vortex wall pairs were significantly distorted such that the regions aligned to the flux-closing monopole field were enlarged, while those that opposed it were reduced in size. That no vortex wall pairs with opposite circulations were observed indicates that the energies of pairs of identical and non-identical vortex walls were not degenerate, and hence that the walls' interaction energy depended on their relative chirality. This correlation between the DW chiralities was reduced for d = 200 nm mirror wires, since vortex wall pairs with identical and opposite chirality were observed [Fig. 2(c)].

For the concentric wires with the lowest spacing (150 nm) strong correlation of the DW structures were observed, with all pairs exhibiting vortex domain walls with opposite circulations [Fig. 2(d)]. However, upon increasing the separations to 200 nm wall pairs with both identical and opposite chirality were observed, again appearing to indicate a reduction in the coupling between the structures of the DWs [Fig. 2(e)]. Finally, in the wires with separations of 500 nm the majority of wall pairs exhibited opposite chiralities [Fig. 2(f)].

Micromagnetic simulations in which DW pairs were inserted into parallel nanowires with a variety of relative displacements, x, were performed to allow a more detailed understanding of the DW interactions [Fig 3(a)]. The interaction energy, E, was calculated as a function of the position of the upper wall while the lower wall remained stationary, and was extracted from the system's total energy by subtracting the energy calculated for isolated domain walls. The DWs' structures were assumed to be rigid, and were either both clockwise vortices (c,c), an anti-clockwise vortex in the upper wire and a clockwise vortex in the lower wire (a,c), or both transverse (t,t). Both walls were H2H to model concentric wires while the wall in the upper wire became T2T for modeling the mirror wire geometry.

For concentric wires with d = 150 nm E increases as the walls are brought together [Fig. 3(b)], as is expected from the walls' monopole repulsion. However, there are subtle differences in the shapes of the (c,c) and (a,c) curves such that for a given wall displacement, one configuration has lower energy. We believe that this effect is the origin of the correlation between DW structures observed experimentally.

The shapes of the curves in Fig. 3(b) can be understood by considering the magnetic pole density distributions within the DWs, which are proportional to $\nabla \cdot \mathbf{M}$ [Fig. 1(b) and (c)] (This definition can be seen to also include surface poles ($\mathbf{n} \cdot \mathbf{M}$) via the divergence theorem). The pole distributions are equivalent to magnetic "charge" distributions and will undergo Coulomb-like interactions with each other. For a vortex wall the charge forms a pair of oppositely oriented triangles bounding the vortex core. At the apex of these triangles edge charge with polarity opposite to the walls' volume charge" is observed, whereas at the flat edge the edge charge is of the same polarity as the volume charge. Reversing the chirality or monopole charge of the DWs causes the shape of the distribution to be reflected about a line along the centre of the nanowire. In the case of the (c,c) vortex walls the charge distributions of the two walls are identical, and hence a positive displacement of the upper wall is not geometrically equivalent to a negative displacement. This causes the shape of the curve to be asymmetric about zero displacement. The interaction energy peaks at negative displacement, where flat edges of the walls' triangular charge distributions are brought together, but is significantly lower at positive displacement, when two apexes are in close proximity. We explain this as follows: The effective charge centre of each half of the DWs will be biased

towards the wider end of the triangular distribution, leading to strong interactions at positive displacements. Contrastingly, at negative displacements the edge charges at triangles' apexes are likely to screen the walls volume charge, reducing the strength of the interaction. For the (a,c) pair the pole density distributions mirror each other and hence movement of the upper wall in either direction is equivalent, creating a symmetric energy landscape.

The peak values of $\partial E/\partial x$ in the curves are proportional to the magnetic fields required to move the upper DW past the lower DW. For the (a,c) wall pair it is predicted that a field of 23 Oe would be required to overcome the DWs' repulsion, whereas for the (c,c) DW pair the asymmetry of the energy landscape means that a larger field (30 Oe) would be required to propagate the upper wall left to right than right to left (21 Oe). These effects are examined in more detail in a separate publication [18].

Similar modeling of mirror wires with 50 nm spacing [Fig. 3(c)] reveals energy minima that represent the attractive monopole interaction for this geometry. The lower energy combination of vortex walls is again dependent on the wall position. Also shown is the interaction energy E for aligned transverse walls, which for zero wall displacement is ~80 % larger than for the vortex walls. This enhancement is most likely due to the transverse walls' magnetizations creating a dipolar field component which strongly couples the walls when they are close together [19]. However, this does not make the (t,t) configuration the ground state at this separation, as demonstrated by the dotted line in Fig. 3(c) which shows E for the (t,t) state offset by the energy cost of having transverse rather than vortex walls in the wires.

Calculations of E for mirror wires with larger separations [Fig. 3(d)] show that the differences between the (c,c) and (a,c) curves are reduced, which reflects the reduced significance of the magnetic pole spatial distribution within the walls. This also explains the reduced experimental correlation between wall structures at larger separations, since the small energy differences between the domain wall states will become less significant relative to the effects of wire defects and thermal excitations.

Fig. 3(e) plots E for the (c,c), (a,c) and (t,t) wall pair states as a function of mirror wire separation, for x = 0. For comparison, a simple monopole model [20] which assumes that the total pole density of the DW is concentrated at its center is also shown. Although at large separations all four curves are in good agreement, at separations <200 nm there is significant lifting of the degeneracy of the energies of the various states indicating that there will be strong coupling between the DW structures and chiralities. Here, the (t,t) interaction energy is much stronger than that predicted by the monopole model, most likely due to the dipolar effects discussed earlier. In contrast to this, E for the vortex walls at low separations is weaker than predicted by the monopole model, perhaps due to the enhanced flux closure that occurs within a vortex wall.

From Fig. 3 it is clear that the wall configuration that is favored by the DW coupling depends on the walls' relative positions. Fig. 4(a) and 4(b) show the energy difference between the (a,c) and (c,c) configurations ($E_{c,c} - E_{a,c}$) as a function of wall separation, for each of the mirror and concentric wire pairs imaged experimentally. In the mirror wires with 50 nm separation the peak value of ($E_{c,c} - E_{a,c}$) is as large as 19 % of the average DW interaction energy. Data for the (t,t) wall pairs is not shown, as these configurations are always meta-stable or unstable for these geometries.

We have used the simulation results to classify the experimentally imaged configurations as meta-stable (i.e. transverse walls), stable and "favorable" by structural coupling, or stable but "unfavorable" by structural coupling. Statistical analysis of the relative frequency of these classifications [Fig. 4(c) and 4(d)] provides compelling evidence of coupling between the magnetic structures of the walls, with the data from the most closely spaced mirror and concentric wire pairs both allowing the rejection at significance level < 0.005 % of a null hypothesis that "favorable" or "meta-stable" states were not formed preferentially. The data also show the decreasing coupling of DW structure for increased wire separation. This is particularly evident for the concentric wires, for which a decreasing number of wall pairs were observed in "favorable" configurations as the separation between the wires is increased, until at d = 500 nm there are an equal number of pairs in "favorable" and "unfavorable" states, showing that there is no statistically significant interaction between DW configurations. A similar trend is observed for mirror wires, where "unfavorable" states are only observed at the widest (200 nm) wire separation.

In conclusion, we have presented unambiguous experimental evidence that inter-wall magnetostatic interactions have significant effects on the behavior of DWs in nanowires. We have observed strong attraction/repulsion between domain walls with opposite/like monopole moments. Furthermore, for wire separations < 200 nm, the domain wall interaction energy additionally depends on the magnetization configuration and chirality of the walls. This manifests as the preferential formation of certain domain wall configurations when the nanowires are relaxed from saturation.

Our findings resolve critical outstanding questions regarding the behavior of domain walls and will have particular implications for technologies based on the propagation of domain walls through nanowire circuits. To avoid crosstalk between neighboring channels, one will not only have to compensate for simple monopole type interactions between walls, but also to take account of the specific wall structures present. Further, systematic investigations are required to fully understand how the strength of these interactions depends on the geometry of the nanowires, and the manner in which the interactions are altered in the dynamic regime where domain wall structure can oscillate [21].

This work was supported by EPSRC (grants GR/T02959/01, EP/F024886/1, EP/F069359/1 and EP/D056683/1) and by the Director, Office of Science, Office of Basic Energy Sciences, Materials Sciences and Engineering Division, of the U.S. Department of Energy.

References

[1] R. D. McMichael and M. J. Donahue, IEEE. Trans. Magn. **33**, 4167 (1997).

[2] S. S. P. Parkin, M. Hayashi and L. Thomas, Science **320**, 190 (2008).

[3] D. A. Allwood, G. Xiong, C. C. Faulkner, D. Atkinson, D. Petit and R. P. Cowburn, Science **309**, 1688 (2005).

[4] M. Laufenberg, D. Backes, W. Bührer, D. Bedau, M. Kläui, U. Rüdiger, C. A. F. Vaz and J. A. C. Bland, L. J. Heyderman F. Nolting, S. Cherifi, A. Locatelli, R. Belkhou, and S. Heun, E. Bauer, Appl. Phys. Lett. **88**, (2006).

[5] P. E. Roy, J. H. Lee, T. Trypiniotis, D. Anderson, G. A. C. Jones, D. Tse, C. H. W. Barnes, Phys. Rev. B. **79**, 060407 (2009).

[6] D. Atkinson, D. A. Allwood, G. Xiong, M. D. Cooke, C. C. Faulkner, and R. P.Cowburn, Nature Mater. **2**, 85 (2003).

[7] G.S.D. Beach, C. Nistor, C. Knutson, M. Tsoi and J.L. Erskine, Nature Mater. **4**. 741 (2005).

[8] N. Vernier, D.A. Allwood, D. Atkinson, M.D. Cooke and R.P. Cowburn, Europhys Lett **65**, 526 (2004).

[9] M. Hayashi, L. Thomas, C. Rettner, R. Moriya, Y. B. Bazaliy, and S. S. P. Parkin, Phys. Rev. Lett. **98**, 037204 (2007)

[10] M. Kläui, H. Ehrke, U. Rüdiger, T. Kasama, R.E. Dunin-Borkowski, D. Backes, L.J. Heyderman, C.A.F. Vaz, J.A.C. Bland, G. Faini, E. Cambril and W. Wernsdorfer, Appl. Phys. Lett. **87**, 102509 (2005).

[11] M. Hayashi, L. Thomas, C. Rettner, R. Moriya, X. Jiang and S. S. P. Parkin, Phys. Rev. Lett. **97**, 207205 (2006).

[12] D. Bedau, M. Kläui, M. T. Hua, S. Krzyk, U. Rüdiger, G. Faini and L. Vila, Phys. Rev. Lett. **101**, 256602 (2008).

[13] M. Laufenberg, D. Bedau, H. Ehrke, M. Kläui, U. Rüdiger, D. Backes, L. J. Heyderman, F. Nolting, C. A. F. Vaz, J. A. C. Bland, Appl. Phys. Lett. **88**, 212510 (2006).

[14] L. O'Brien, D. Petit, H. T. Zeng, E. R. Lewis, J. Sampaio, A. V. Jausovec, D. E. Read, and R. P. Cowburn., Phys. Rev. Lett. **103**, 077206 (2009).

[15] P. Fischer, T. Eimüller, G. Schütz, G. Denbeaux, A. Pearson, L. Johnson, D. Attwood, S. Tsunashima, M. Kumazawa, N. Takagi, M. Köhler and G. Bayreuther, Rev. Sci. Instr. **72(5)**, 2322 (2001).

[16] P. Fischer, D.-H. Kim, W. Chao, J. A. Liddle, E. H. Anderson, and D. T. Attwood, Mater. Today **9**, 26 (2006).

[17] http://math.nist.gov/oommf/

[18] T.J. Hayward, M.T. Bryan, P.W. Fry, P.M. Fundi, M.R.J. Gibbs, D.A. Allwood, M.-Y. Im and P. Fischer, to be published in Applied Physics Letters.

[19] The reader can reconcile this dipolar coupling with the Coulomb-like interaction picture used earlier by realizing that this orientation of transverse walls brings together large edge charges of opposite polarity.

[20] $E_{\cdot} = q_i q_j / 4\pi\mu_0 r$, where $q = \pm 2\mu_0 Mwt$ is an analytically derived value of DW's net magnetic "charge" (+ H2H, - T2T) and r is the distance between the DWs. M represents the saturation magnetization of $Ni_{80}Fe_{20}$, while w and t are the nanowires' thickness and width respectively.

[21] M.T. Bryan, T. Schrefl, D. Atkinson and D.A. Allwood, J. Appl. Phys. **103**, 073906 (2008).

Figure Captions

Fig. 1: (Color online) (a) Schematic diagrams of a head-to-head and a tail-to-tail DW. (b) Magnetization structure (**M**) and magnetic pole density plot ($\nabla \cdot \mathbf{M}$) produced from a micromagnetic simulation of a vortex wall. (c) **M** and $\nabla \cdot \mathbf{M}$ plots for a transverse wall. (d) Schematic diagram and scanning electron microscopy (SEM) image showing the "mirror" wire pair geometry. (e) The "concentric" wire pair geometry.

Fig. 2: (Color online) (a)-(c) M-TXM images of DW configurations observed in the "mirror" geometry wires. Micromagnetic simulation results showing a pair of coupled transverse walls and a pair of vortex walls distorted by the magnetic field closing between the walls are also shown in (a) and (b). (d)-(f) M-TXM images showing domain wall configurations observed in the "concentric" geometry wires.

Fig. 3: (Color online) (a) Geometry simulated to measure the interaction energy, *E*, between DW pairs. (b) *E* as a function of wall displacement for concentric wires with spacing, d = 150 nm. The data are offset by the interaction between the wires' end domains. (c) Equivalent plot for a pair of mirror wires with d = 50 nm. The dashed line shows the (t,t) data offset by the energy cost of having transverse, rather than vortex walls in the nanowires. (d) *E* for mirror wires with separations of 50 nm (circles), 100 nm (squares) and 200 nm (triangles) for (c,c) DW pairs (open symbols) and (a,c) DW pairs (filled symbols) . (e) *E* as a function of wire pair separation for zero wall displacement. Data are also shown for a simple monopole model.

Fig. 4: (Color online) (a) Interaction energy difference between (a,c) and (c,c,) configurations, $E_{a,c}$-$E_{c,c,}$ as a function of wall displacement for the mirror wire geometry with 50 nm (circles), 100 nm (diamonds) and 200 nm (triangles) spacing. The dashed line shows approximately where $E_{a,c}$-$E_{c,c}$ = 0. (b) Equivalent plot for the concentric wire geometry with 150 nm (circles), 200 nm (diamonds) and 500 nm (triangles) spacings. (c) and (d) Frequency of the experimentally observed DW configurations: stable and favored by DW coupling (filled); stable and unfavorable by DW coupling (unfilled); and meta-stable transverse wall pairs (hashed).

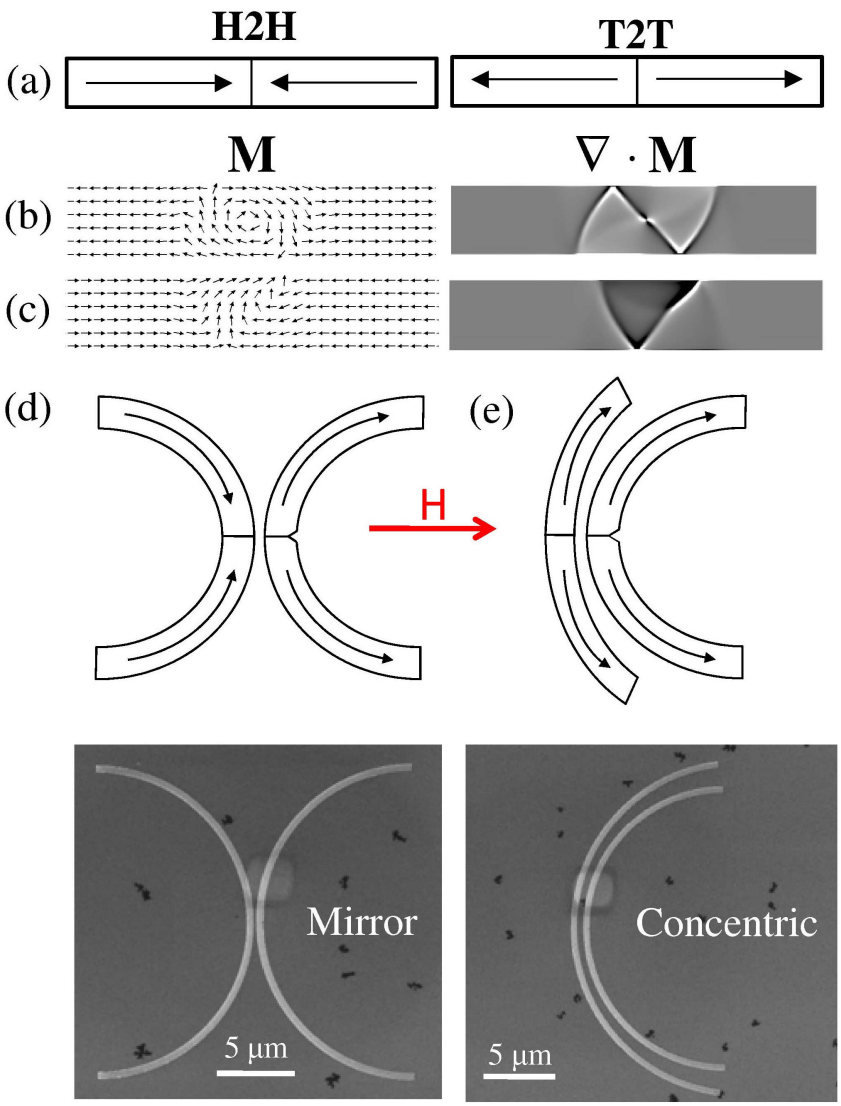

Figure 1

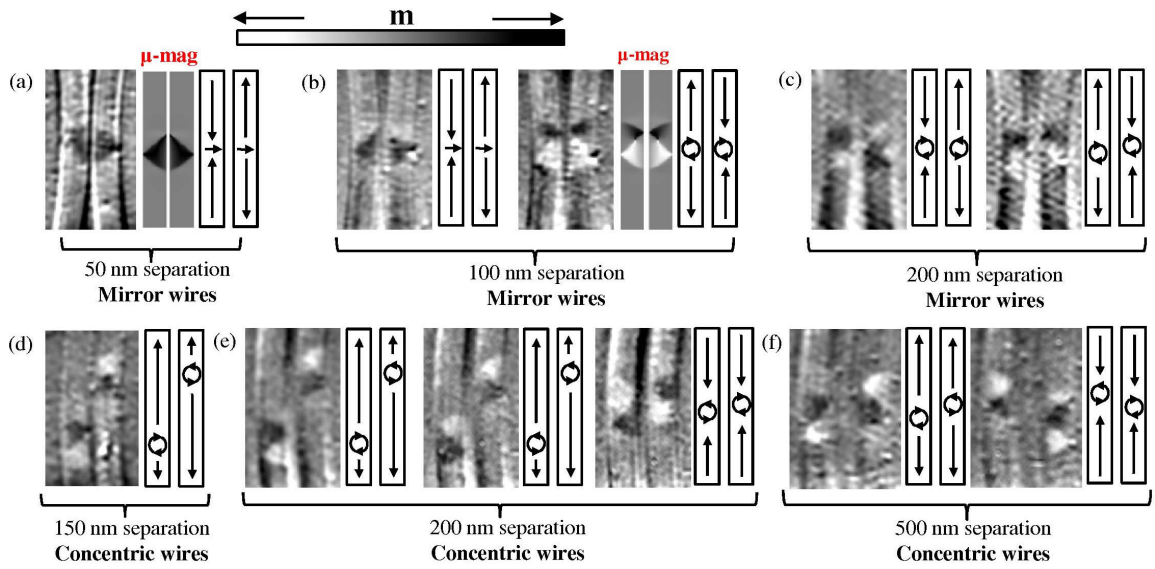
m
μ-mag
μ-mag
(a)
(b)
(c)
50 nm separation
Mirror wires
100 nm separation
Mirror wires
200 nm separation
Mirror wires
(d)
(e)
(f)
150 nm separation
Concentric wires
200 nm separation
Concentric wires
500 nm separation
Concentric wires

Figure 2

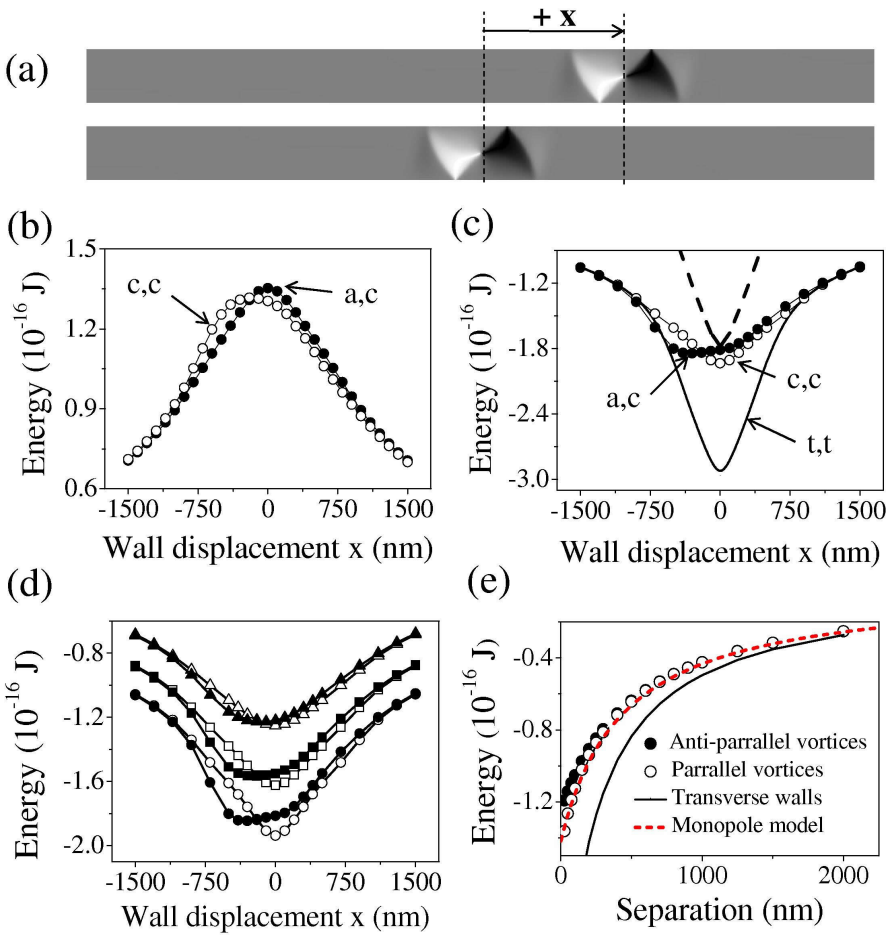
(a)
+ x
(b)
Energy (10^{-16} J)
1.5
1.2
0.9
0.6
c,c
a,c
-1500 -750 0 750 1500
Wall displacement x (nm)
(c)
Energy (10^{-16} J)
-1.2
-1.8
-2.4
-3.0
a,c
c,c
t,t
-1500 -750 0 750 1500
Wall displacement x (nm)
(d)
Energy (10^{-16} J)
-0.8
-1.2
-1.6
-2.0
-1500 -750 0 750 1500
Wall displacement x (nm)
(e)
Energy (10^{-16} J)
-0.4
-0.8
-1.2
Anti-parrallel vortices
Parrallel vortices
Transverse walls
Monopole model
0 1000 2000
Separation (nm)

Figure 3

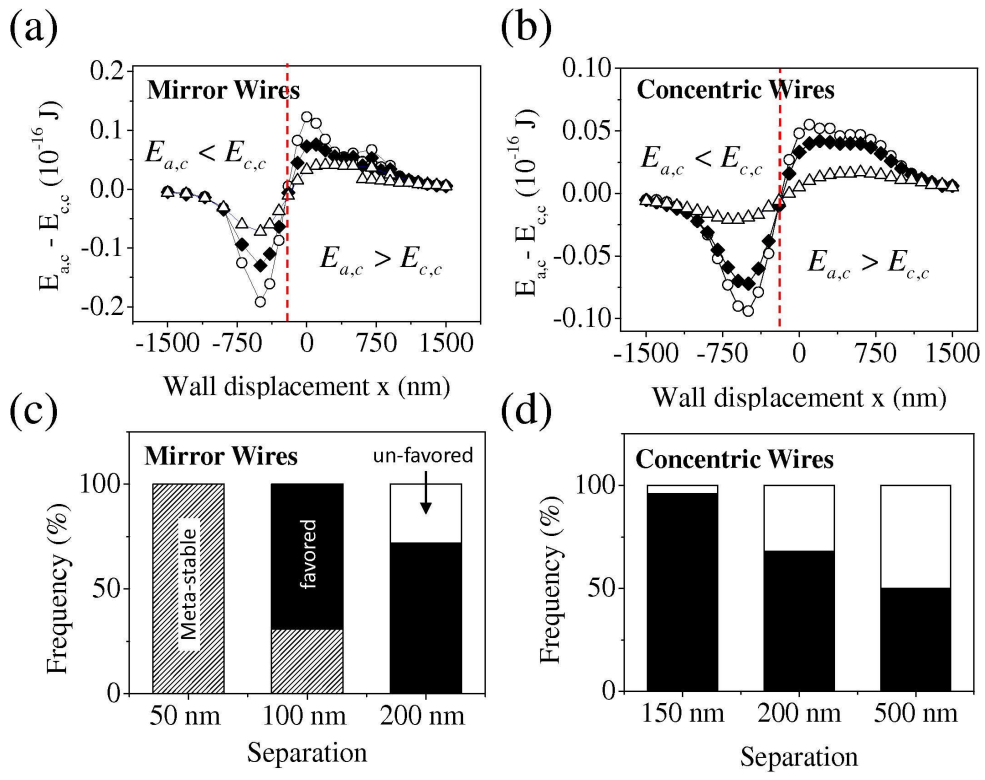
(a)
Mirror Wires
$E_{a,c} < E_{c,c}$
$E_{a,c} > E_{c,c}$
$E_{a,c} - E_{c,c}$ (10^{-16} J)
Wall displacement x (nm)
(b)
Concentric Wires
$E_{a,c} < E_{c,c}$
$E_{a,c} > E_{c,c}$
$E_{a,c} - E_{c,c}$ (10^{-16} J)
Wall displacement x (nm)
(c)
Mirror Wires
un-favored
Meta-stable
favored
Frequency (%)
50 nm
100 nm
200 nm
Separation
(d)
Concentric Wires
Frequency (%)
150 nm
200 nm
500 nm
Separation

Figure 4